5
SICL based multi-functional components and six-port network

The unprecedented growth and utilization of wireless services provided by portable hand-held user equipment (UE) has extended usage for consumers. These hand-held devices are required to have small size, low weight, consume less power and affordable in terms of cost (SWaP-C). Utilization of multifunctional components in the current radio transceivers aids in realizing SWaP-C. The multi-functionality is brought into a single component by that serves the functionality of two or more components to save crucial on-board space and ultimately reduces cost. Further, multi-functional components eliminates the need for interface between the two different circuits and hence reduces impedance mismatch and improves the overall performance of the system. Steadily growing modern communication requires transition to multi-functional components for enhanced operation of RF-front end. The initial blocks of any typical receiver comprises of antenna followed by a bandpass filter. Antenna receives the electromagnetic signal from the unguided media and the bandpass filter selects the desired band of frequencies for further processing. Instead of cascading these two front-end components, design of a single component that can serve the functionality of antenna and filter is highly desirable as it can keep the receiver compact and deliver good performance. Another challenge in design of a transceiver is the integration of various RF-front end components. The transmitter and receiver section in transceiver is integrated with a single antenna using a diplexer. Diplexer is a three port network that separates the transmitting and receiving signal on the basis of the frequency of operation. Diplexers are required to have low insertion loss, high selectivity for enhanced utilization of spectrum and excellent isolation between the transmitting and receiving channels to avoid any undesirable interference. Diplexer integration with antenna makes the first step in design of a RF-front end. Another architecture that is popular in receivers is six port network. First conceived as a tool for power measurement and calibration, the six port network later gained importance in determination of direction of arrival of EM wave, passive mixer, microwave imaging and for many more such application.

This chapter begins with the design of a filtenna, an antenna integrated with bandpass filter. The proposed SICL based multi-functional component demonstrating both radiating and filtering function is realized by integrating parallel coupled bandpass filter with a slot antenna. The design, development and integration of fiter-antenna system is discussed in detail. Later, a highly selective diplexer with excellent isolation and multiple transmission zeros is synthesized. The proposed SICL diplexer is conceived using two bandpass filters and an impedance matching network. A high gain linearly tapered antipodal antenna fed by GCPW line is realized. The integration of the proposed diplexer with a high gain antenna is demonstrated in this work. Finally, using the wideband branch line coupler and wideband wilikinson power divider discussed in previous chapter, a SICL based six-port module is developed. The proposed wideband six-port network works over the entire K_u band and is realized in a compact form factor. Such six-port are very useful in realizing various receiver architectures.

5.1 CO-DESIGN OF A SUBSTRATE INTEGRATED COAXIAL LINE FILTER-ANTENNA FOR MILLIMETER-WAVE APPLICATIONS

The demand for light weight and small form-factor communication systems motivates further investigation in to the basic building blocks of RF front-end architecture. In a transceiver, one of the first components than an EM signal from unguided media interacts with are the antenna and filter. The following work develops a design approach to synthesize a substrate integrated coaxial line (SICL) based filter-antenna for the millimeter-wave band.

5.1.1 Design of 5^{th} order SICL based parallel coupled BPF

The physical layout and stack-up of the proposed parallel-coupled SICL BPF is shown in Fig. 5.1. The design of the proposed 5^{th} order BPF starts with developing a chebyshev filter of 0.5 dB ripple. The parameters of the low-pass prototype [130] and characteristic admittance of J-inverter [80] to cover a fractional bandwidth (FBW) of 12.01% at center frequency 28.3 GHz are calculated using (5.1)-(5.3) & listed in Table 5.1.

$$\frac{J_{01}}{Y_o} = \sqrt{\frac{\pi}{2}\frac{FBW}{g_o g_1}} \tag{5.1}$$

$$\frac{J_{j,j+1}}{Y_o} = \frac{\pi FBW}{2}\frac{1}{\sqrt{g_j g_{j+1}}} \quad \text{for } j = 1 \text{ to } n-1 \tag{5.2}$$

$$\frac{J_{n,n+1}}{Y_o} = \sqrt{\frac{\pi}{2}\frac{FBW}{g_n g_{n+1}}} \tag{5.3}$$

The synthesized insertion loss plot for proposed specification is shown in Fig. 5.2(a). The design of proposed BPF in SICL technology starts with the determination of characteristic impedance of SICL line. Using the theoretically synthesized filter information, the width of SICL resonators

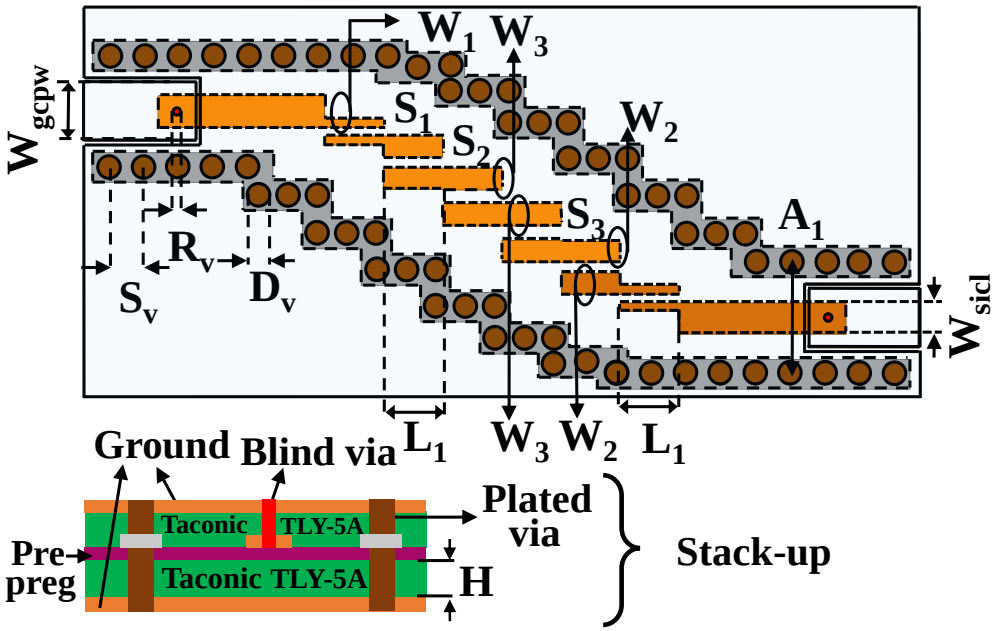

Figure 5.1 : Geometrical layout of the proposed 5^{th} order SICL based parallel-coupled BPF with dimensions: A_1 = 3mm, D_v = 0.6mm, R_v = 0.2mm, S_1 = 0.22mm, S_2 = 0.28mm, S_3 = 0.38mm, S_v = 0.8mm, L_1 = 1.6, W_1 = 0.24mm, W_2 = 0.58mm, W_3 = 0.6mm, W_{gcpw} = 1.6mm, W_{sicl} = 0.86mm.

Table 5.1 : Computed J-inverter admittance and even/odd mode impedances of the coupled lines

j	g_{j+1}	$J_{j,j+1}/Yo$	$(Z_{0e})_{j,j+1}$	$(Z_{0o})_{j,j+1}$
0	1.7058	0.3326	72.1577	38.9018
1	1.2296	0.1303	57.3615	44.3353
2	2.5408	0.1067	55.9062	45.2330
3	1.2296	0.1067	55.9062	45.2330
4	1.7058	0.1303	57.3615	44.3353
5	1.000	0.3326	72.1577	38.9018

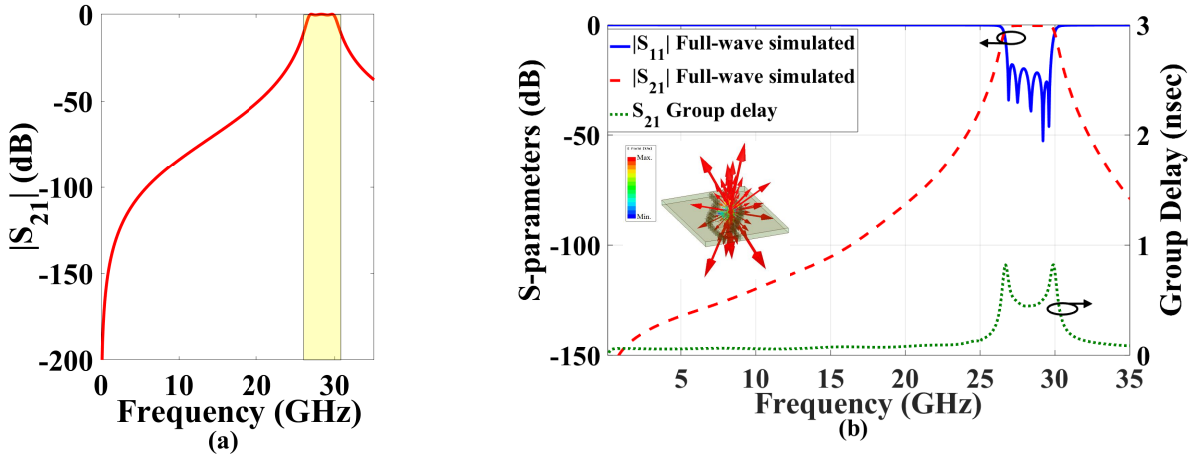

Figure 5.2 : Broadband bandpass filter design (a) Theoretically synthesized $|S_{21}|$ of a 5^{th} order parallel coupled BPF (b) Full-wave simulated S-parameters and group delay of the proposed SICL based broadband BPF.

and spacing between them is determined through full-wave simulator Ansys HFSS. SICL is a two conductor transmission line. The lateral metallic vias along with bottom and top ground plane form outer conductor, whereas the metallic strip sandwiched between the substrate makes the inner conductor of this planar dielectric filled coaxial line. The coaxial like radially outward directed E-field vector and concentric H-field in SICL transmission line are confirmed using Ansys HFSS and their field distribution has been shown in Fig. 1.5. In inset of Fig. 5.2 (b), the radially outward E-field in proposed SICL filter exhibits field distribution similar to that of traditional coaxial line [92]. Simulated performance of proposed SICL based broadband filter in Fig. 5.2(b) demonstrates return loss better than 18 dB, insertion loss less than 0.78 dB & a group delay deviation of 0.4 nsec over 26.6 GHz to 30 GHz band. The self-packaged SICL structure is electromagnetically robust as the inner conductor sandwiched between a pair of dielectrics is covered with an outer conductor formed by top and bottom ground planes along with electroplated via holes.

5.1.2 Fabrication & measurement of proposed SICL based bandpass filter

To validate the proposed filter synthesis, the SICL based 5^{th} order parallel coupled bandpass filter is fabricating using pair of Taconic TLY-5A (ε_r = 2.2, δ = 0.0009) substrate, each of thickness 0.508 mm bonded with Taconic FR-28 prepreg (ε_r = 2.74, tanδ = 0.0014) of 4 mil thickness. The photograph of the fabricated prototype depicting its top and bottom view with connectors

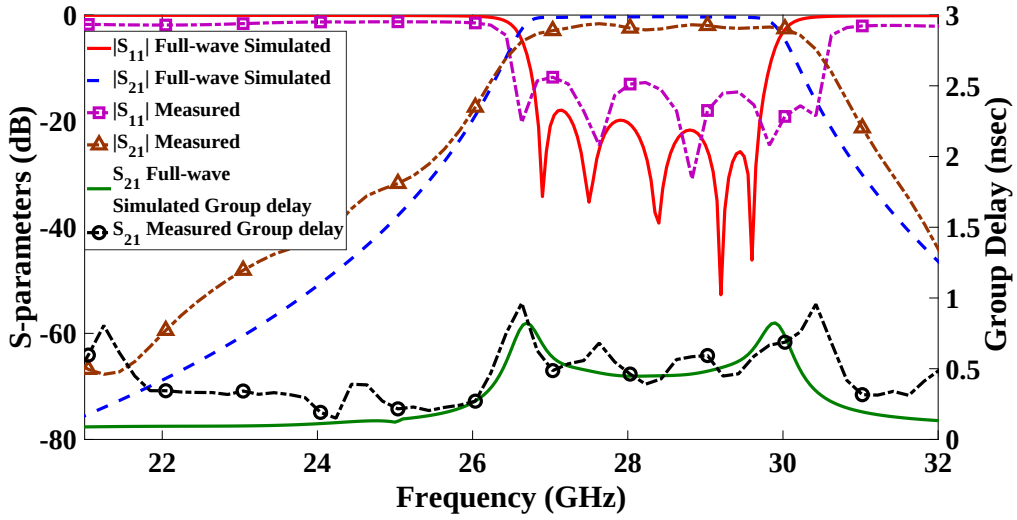

Figure 5.3 : Comparison between full-wave simulated and measured S-parameters of the proposed SICL based bandpass filter.

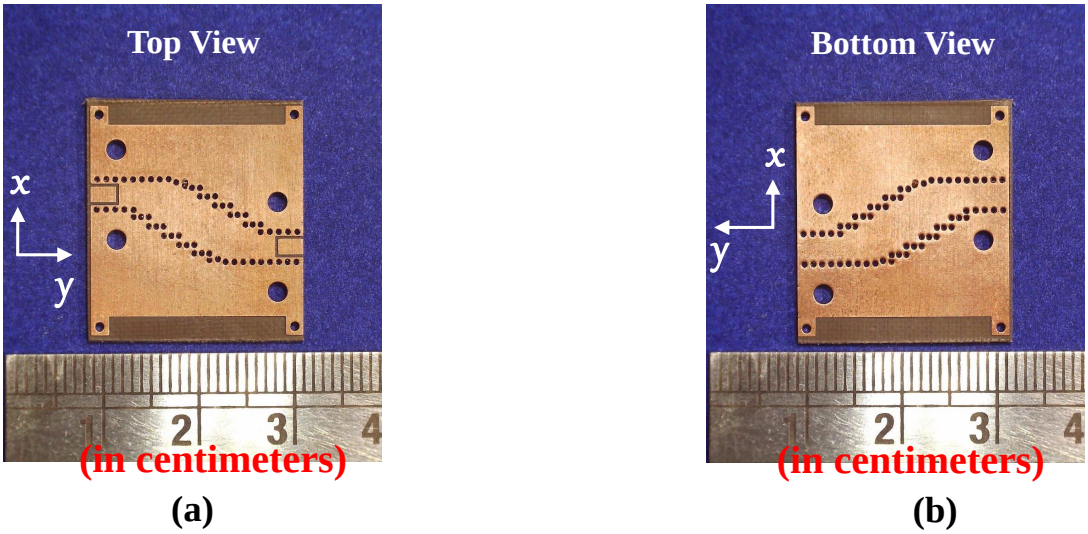

Figure 5.4 : Photograph of fabricated prototype of the proposed dual-mode SICL cavity filter.

are shown in Fig. 5.4. The full-wave S-parameters computed using Ansys HFSS are affirmed by recording the S-parameters of proposed prototypes using Agilent N5234A (10 MHz to 43.5GHz) vector network analyzer as shown in Fig. 5.3. The, measured results of proposed SICL bandpass filter demonstrates an insertion loss of 1.96 dB at the center frequency 28 GHz with a 3-dB fractional bandwidth of 14.03%. The deviation in measured filter response maybe attributed to fabrication tolerance and minor air-gaps between the stacked dielectric substrates.

5.1.3 Integration of filter-antenna in SICL technology

The proposed SICL filter-antenna with dimensions is shown in Fig. 5.1(a). Co-design of proposed SICL based filter-antenna starts with short-circuiting the SICL based BPF to the via holes connecting the top and bottom ground plane. A rectangular slot inclined at 135° is etched at the

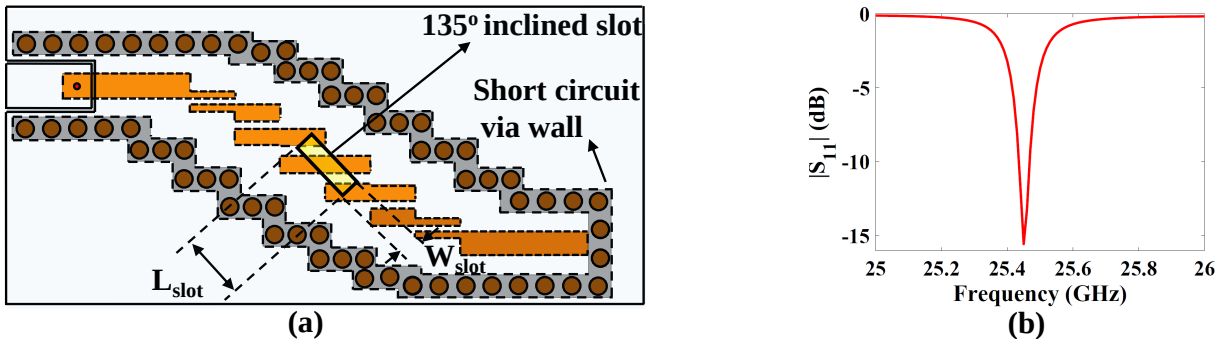

Figure 5.5 : Proposed SICL based filter-antenna (a) Geometrical layout of the proposed filtenna with dimensions: L_{slot} = 2.9mm, W_{slot} = 0.65mm (b) Reflection coefficient

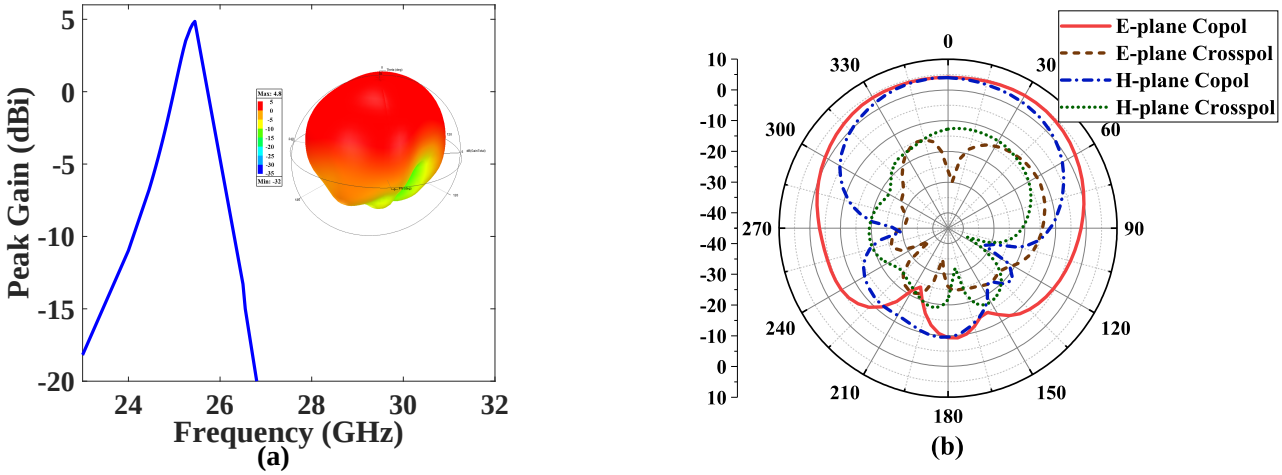

Figure 5.6 : Radiation characteristics of proposed SICL based filter-antenna system (a) Peak gain (b) E- and H-plane radiation pattern at 25.45 GHz.

center of top ground plane. The proper orientation of slot controls the coupling between slot and SICL resonator. The TEM based SICL resonator appropriately excites the slot to radiate in free space. The proposed filter-antenna system radiates a peak gain of 4.8 dBi with good filtering characteristics affirmed by sharp roll-off rate as shown in Fig. 5.6(a). The 3D-radiation pattern depicted in inset of Fig. 5.6(a) demonstrates a unidirectional pattern owing to the bottom ground plane acting as a reflector. The simulated radiation pattern recorded in E-plane and H-plane is depicted in Fig. 5.6(b).

5.1.4 Simulation results

A pair of Taconic TLY-5A (ε_r = 2.2, tan δ = 0.0009) substrate each of thickness 0.5 mm are bonded together with Taconic FR-28 (ε_r = 2.7, tan δ = 0.003) for the design of proposed SICL based filter-antenna. The full-wave simulated reflection coefficient analyzed using Ansys HFSS is shown in Fig. 5.5(b). The position of rectangular slot disturbs the current path and loading effect produced by short-circuited SICL resonator shifts the resonant frequency of proposed filter-antenna to 25.45 GHz. A 10-dB narrow impedance bandwidth of 30 MHz is noted at the center frequency. The ground plane backed slot antenna demonstrates a front to back ratio of 14.36 dB and co-pol to cross-pol ratio better than 34 dB and 18 dB, respectively.

5.2 DESIGN AND DEVELOPMENT OF SICL BASED DIPLEXER-ANTENNA SYSTEM

The modern day full-duplex transceivers make use of diplexers to utilize single antenna for both transmitting and receiving channels. The frequency division duplex (FDD) scheme is popular in GSM and WCDMA based cellular communication. In order to make the most of the available spectrum, designers are pushed to build highly selective diplexers with very high isolation to suppress interference between the transmitting and receiving channels. The high isolation reduces the power requirement in receiver chain and allows deployment of low-power receivers with better linearity. Traditionally diplexers were built in waveguide technology [189], as they possess excellent thermal stability and feature loss which highly suitable for satellite communication. However, installation of diplexers in hand-held devices would require compact form-factor. The progress in PCB technologies has enabled manufacturing of microwave & millimeter circuits using ultra thin single and multi-layer substrates. Microstrip diplexers [190, 191] have found universal acceptance for usage in customer premise equipment (CPE) and other forms of portable systems. Low profile SIW based diplexers [192] is used for installation in on the move user equipment for satellite communication (SATCOM) systems. There is an evident need to move to a different technology to combat the shortcoming of semi-open microstrip based diplexers in densely integrated circuits, and large footprint based SIW diplexer in compact systems. In the recent times 3D printed technology [193] has been explored for design of high frequency millimeter based diplexers to support intricate geometries with high quality factor. The following work discusses the design and fabrication of SICL based diplexer for satellite bands with very high isolation in compact size. Furthermore, the proposed diplexer also demonstrates design for excellent out of band suppression.

5.2.1 Modeling of SICL bandpass filters for transmitter and receiver section of diplexer using via-based perturbation technique

The physical layout of via-based bandpass filter for transmitter and receiver section of diplexer is shown in 5.7. The bandpass filter comprises of a ring-shaped uniform impedance resonator (UIR) located between two substrates of same dielectric constant as discussed in section

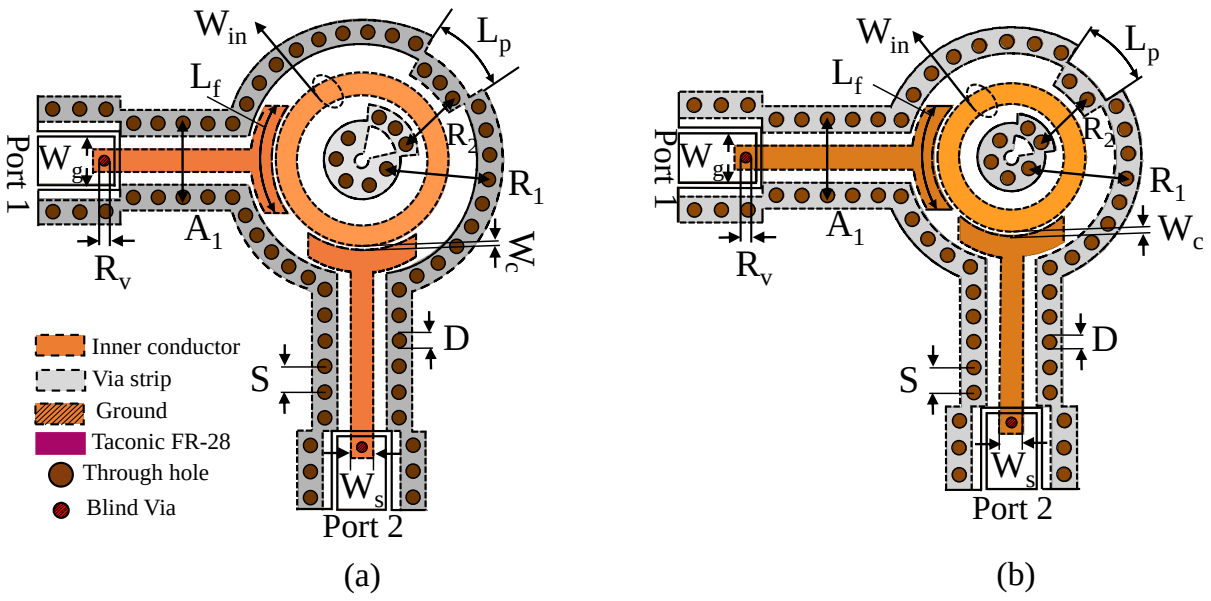

Figure 5.7 : Layout of individual bandpass filters operating at (a) 11.25 GHz for transmitter section (b) 13.8 GHz for receiver section.

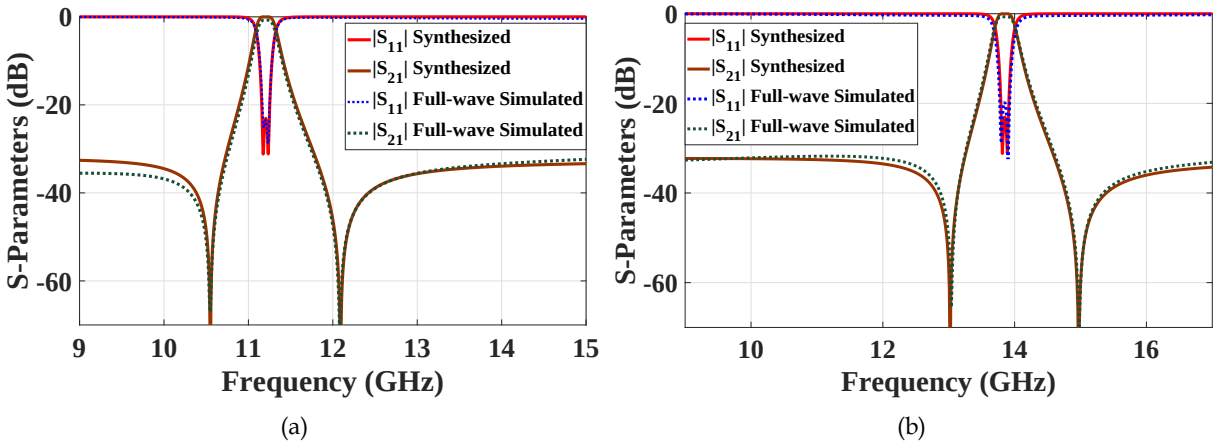

Figure 5.8 : Comparison between synthesized and full-wave simulated S-parameters of bandpass filters operating at (a) 11.25 GHz for transmitter section (b) 13.8 GHz for receiver section.

Table 5.2 : Dimensions of the designed SICL based bandpass filters for transmitter and receiver channel

Parameter	f_c = 11.25 GHz, value (mm)	f_c = 13.8 GHz, value (mm)
A_1	2.75	2.75
D	0.5	0.5
L_f	4.38	4.03
L_p	2.45	1.97
S	0.92	0.92
R_1	3.90	3.5
R_2	2.43	2.26
R_v	0.36	0.36
W_c	0.14	0.14
W_{in}	0.78	0.78
W_s	0.85	0.85

3.1 of chapter 3. SICL is a two conductor transmission line. Electroplated through holes connect the top and bottom ground plane to form is single shielded outer conductor, whereas the metallic strip sandwiched between the substrate makes the inner conductor of this planar dielectric filled coaxial line. The coaxial like radially outward directed E-field vector and concentric H-field in SICL transmission line are confirmed using Ansys HFSS and their field distribution has been shown in Fig. 1.5. The shielding aids in minimization of interference with neighboring components in system. To ensure good shielding the ratio of spacing between vias to pitch of vias is maintained less than 2.5. The SICL based ring resonator is excited using feed lines that are orthogonally placed to each other. A perturbation in the form of offset of vias is introduced at $3\lambda_g/8$ from the feeding location. The length of this perturbation is L_p and depth of inset is denoted by R_2 as shown in Fig. 5.7. Owing to the small width of inner conductor to height of substrate ($W_{in}/2H$) ratio, the via based perturbation changes the characteristic impedance of SICL section over the length L_p. In

the proposed design a planar coaxial line (SICL) is modeled using a conducting strip and series of delimiting vias acting as inner and outer conductor respectively. Due to the change in width of the outer conductor, the characteristic impedance of SICL section is changed over the length L_p, forming a coaxial stepped impedance resonator in planar form.

$$M = \begin{bmatrix} & S & 1 & 2 & L \\ S & 0 & -0.9258 & 0.8766 & -0.0120 \\ 1 & -0.9258 & -1.8586 & 0 & 0.8995 \\ 2 & 0.8766 & 0 & 1.6472 & 0.9007 \\ L & -0.0120 & 0.8995 & 0.9007 & 0 \end{bmatrix} \tag{5.4}$$

The proposed dual-mode filters for 11.2 GHz and 13.85 GHz are synthesized with the help of coupling matrix developed from the coupling scheme in [92]. The two transmission zeros not only provide sharp rejection to the filter but also aid in deep spurious signal suppression of better than 30 dB on lower and upper side of the passband. The detailed design and analysis of the via perturbation based SICL bandpass filter is discussed in detail in section 3.1 of chapter-3.

5.2.2 Design and experimental validation of proposed SICL based high isolation diplexer using impedance transformer

The proposed diplexer design starts with modeling of impedance transformer connects the transmitter and receiver section bandpass filters in order to provide good impedance matching at both band while maintaining high isolation. The traditional T-junction power divider with 50 Ω input impedance at 11.25 GHz/ 13.8 GHz is not suitable as it will produce an mismatch at the junction. Two single section impedance transformers have been employed to feed the two bandpass filters. The left section of the diplexer is connected to a bandpass filter operating at 11.2 GHz and the right section of diplexer is connected to a bandpass filter with passband centered at 13.85 GHz. A T-type impedance transformer is designed by choosing suitable electrical length (L_{imn1} and L_{imn2}) and the characteristic impedance (W_{imn1} and W_{imn2}) such that while the left section of diplexer is operational at 11.2 GHz, a very high impedance is observed looking into the right section of the diplexer. Similarly when the right section of diplexer is operating at 13.85 GHz, a very high

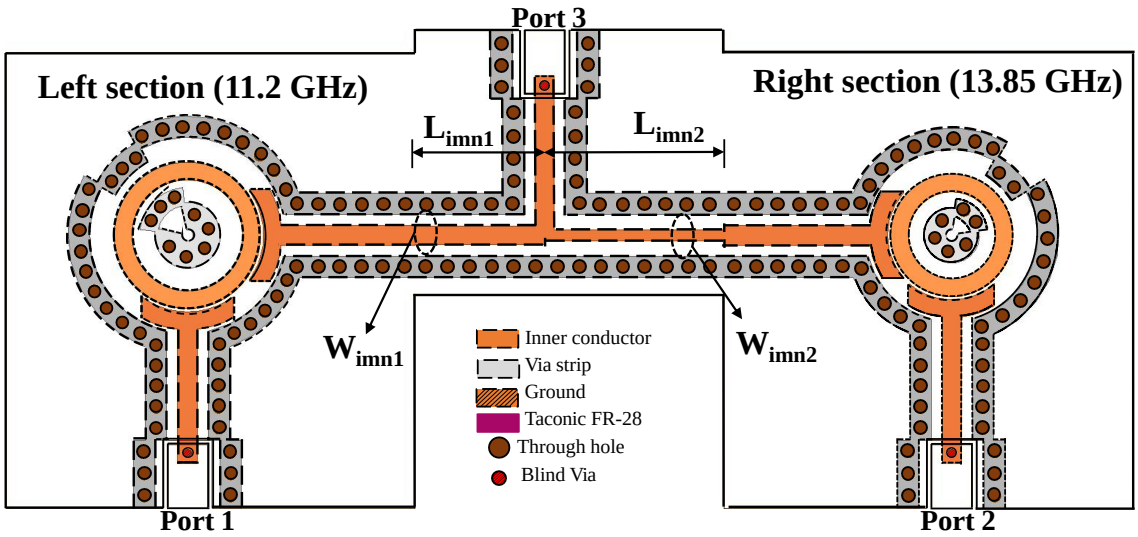

Figure 5.9 : Geometrical layout of the proposed SICL diplexer comprising of two bandpass filter and an impedance transforming section with dimensions: L_{imn1} = 5.7mm, L_{imn2} = 7.9mm, W_{imn1} = 0.8mm and W_{imn2} = 0.5mm.

impedance is observed looking into the left section of the diplexer. The geometrical layout of the proposed SICL diplexer comprising of two bandpass filter and impedance transforming section is shown in Fig. 5.9. To validate the proposed SICL based diplexer synthesis, an experimental prototype is fabricated using two layers of Taconic TLY-5 (ε_r = 2.2, tanδ = 0.0009) of thickness 0.508 mm and bonded together with prepreg Taconic FR-28 (ε_r = 2.82). The photograph of the fabricated SICL diplexer depicting its top and bottom view is shown in Fig. 5.10. The full-wave S-parameters determined using Ansys HFSS are confirmed with the S-parameters of measured prototype using Agilent E5071C vector network analyzer as shown in Fig. 5.11. In Fig. 5.11(a), fabricated SICL diplexer shows a measured return loss better than 15 dB at both the transmitter and receiver bands. Utilization of highly selective filters with selectivity as high as 106.2 dB/GHz [92] and multiple transmission zeros aids in achieving steep rejection skirt and excellent out of band rejection as shown in 5.11(b). Further, the proposed diplexer exhibits low insertion loss of 1.33 dB and 1.58 dB at the center frequency 11.2 GHz and 13.8 GHz respectively as depicted in Fig. 5.11 (b) and (c). Owing to the multiple transmission zeros and self-shielded structure the proposed SICL diplexer demonstrates high isolation of more than 45 dB at transmit and receive frequency bands as shown in Fig. 5.11(c).

5.2.3 Design of GCPW fed Antipodal-Linearly Tapered Slot Antenna on Multi-layered Substrate

The proposed multi-layered ALTSA antenna comprises of three sections, i) GCPW line, ii) SIW section and iii) Antipodal-Linearly Tapered Slot Antenna (ALTSA). GCPW transmission line is utilized to feed the antenna and mount the SMA connector for testing. The 50Ω characteristic impedance GCPW transmission with signal line of width 1.78mm and gap 0.2mm is flared outwards to a width 9.8mm ensuring a smooth transition from TEM mode of GPCW to TE_{10} mode of SIW. The multi-layered SIW section is designed with a total substrate thickness 1.016 mm to support propagation TE_{10} above 10 GHz. The pitch and diameter are chosen such that the s/d ratio is than 2.5 to avoid any wave leakage through the vias. The cut off frequency of SIW for TE_{10} mode of propagation is calculated [23] using equation (5.5)

$$f_c = \frac{c}{2w_{eff}} \tag{5.5}$$

where w_{eff} is the effective width of rectangular waveguide with same propagation characteristics [178]

$$w_{eff} = w - 1.08\frac{d^2}{s} + 0.1\frac{d^2}{w} \tag{5.6}$$

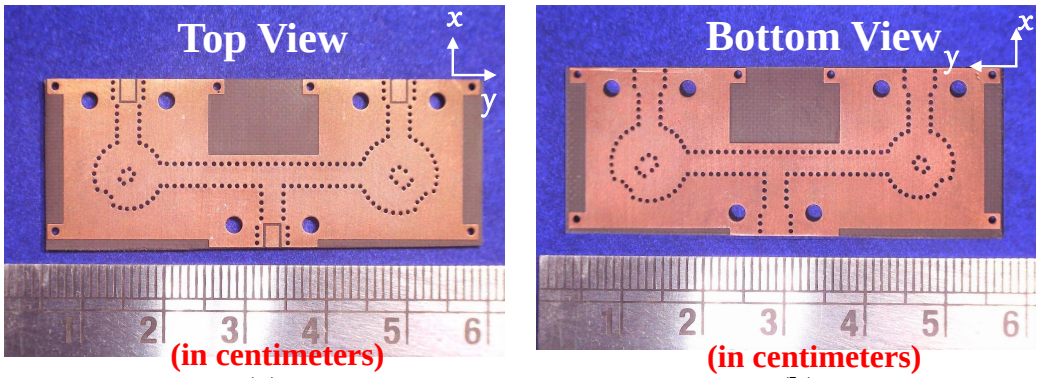

Figure 5.10 : Photograph of the proposed high isolation SICL based diplexer prototype.

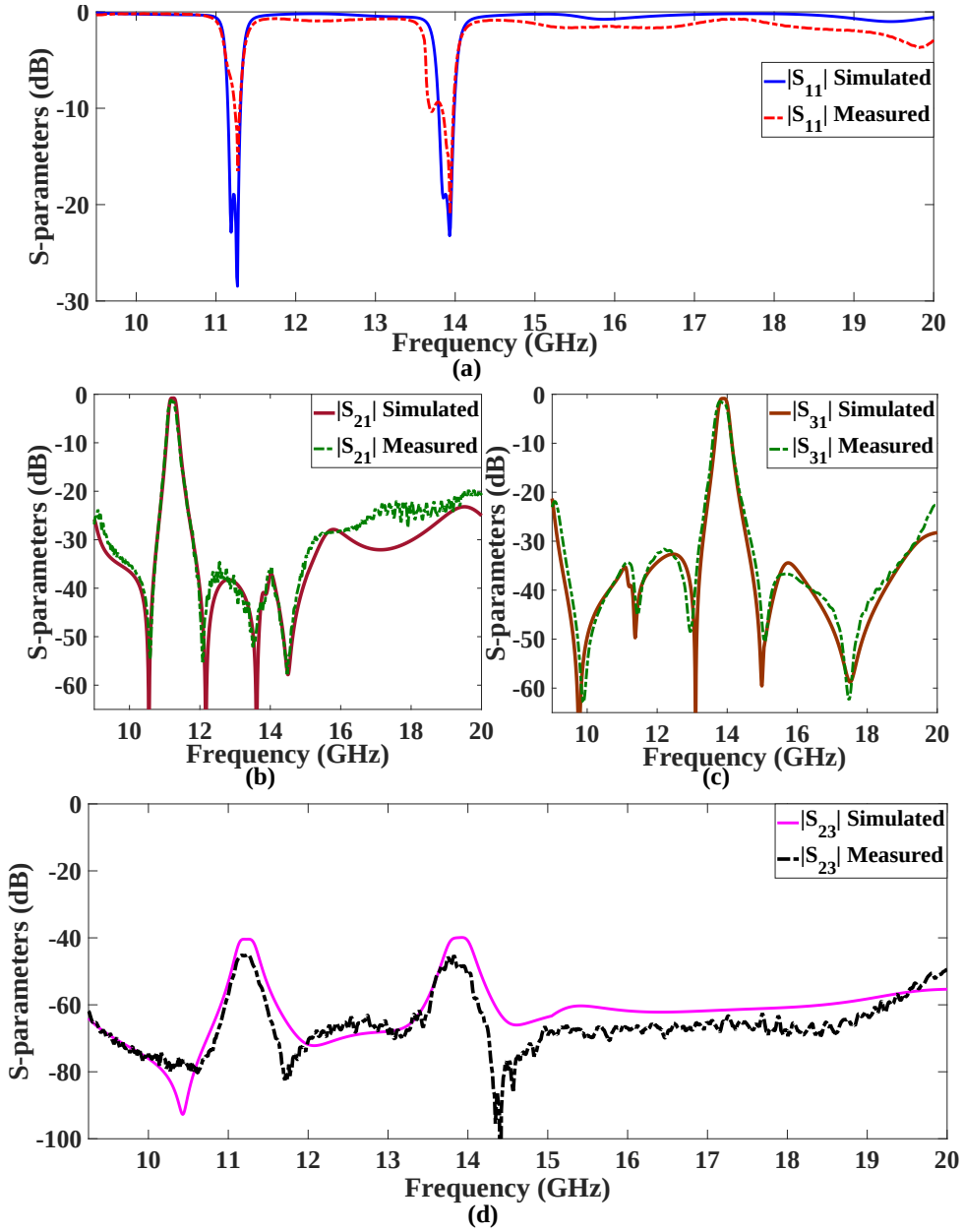

Figure 5.11 : Comparison between full-wave simulated and measured results of the proposed SICL based high isolation diplexer (a) Reflection coefficient (b) & (c) Insertion loss (c) Isolation.

The proposed multi-layered ALTSA antenna in PCB technology is realized through two triangular shaped flared metal strips on the top and bottom side of the substrate as shown in Fig. 5.12. The empirical design rules [194] are given as (5.7) and (5.8). The distance between the two triangularly flared fins of the ALTSA is maintained greater than $\lambda/2$ and the ratio of thickness of substrate to wavelength is kept between 0.005 and 0.03 to ensure good radiation characteristics of ALTSA.

$$W_o \geq \lambda_0/2 \tag{5.7}$$

$$0.005 < \frac{t_{\text{eff}}}{\lambda_0} < 0.03 \tag{5.8}$$

Rectangular corrugations on edges are employed to reduce the cross-polarization level and improve the return loss of the antenna [194]. In this work, the proposed multi-layered ALTSA

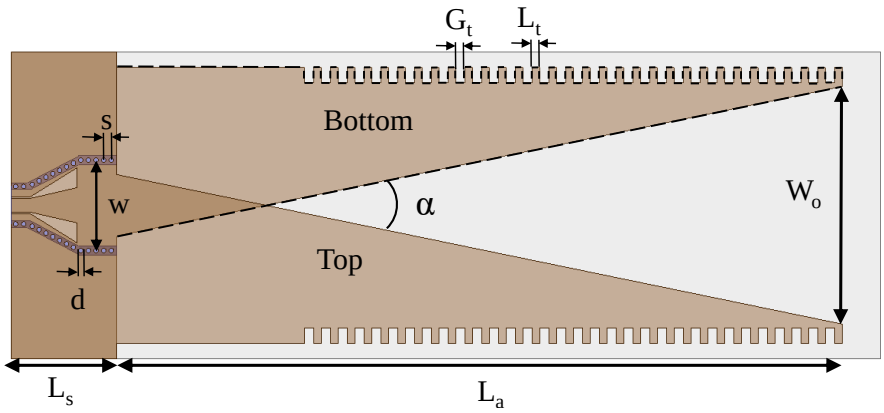

Figure 5.12 : Geometrical Layout of SIW fed antipodal linearly tapered slot antenna (ALTSA).

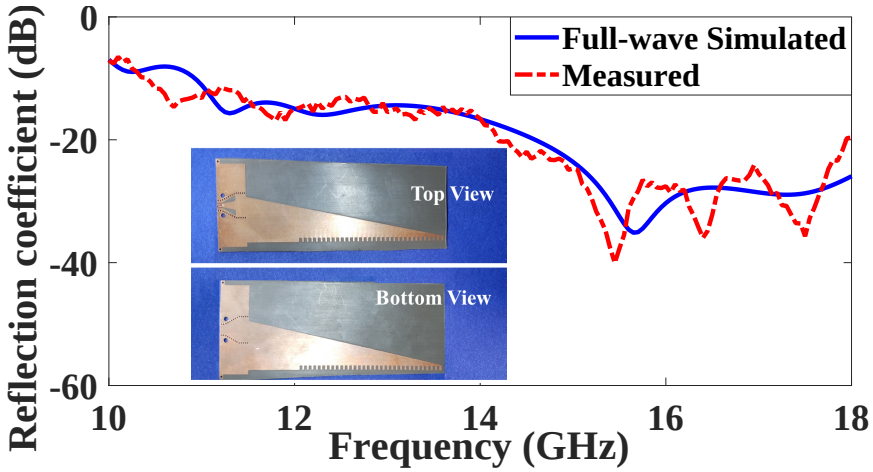

Figure 5.13 : Measured reflection coefficient and photograph of the fabricated SIW fed antipodal linearly tapered slot antenna (ALTSA).

is designed to integrate with the proposed SICL based diplexer. The parameters of the antenna are given as d = 0.6mm, s = 1 mm, G_t = 1.2mm, L_a = 95mm, L_s = 13.85mm, L_t = 1mm, w = 11.8mm, W_o = 31.02mm, α = 16.51°. The photograph of the fabricated multi-layered GCPW fed ALTSA depicting its top and bottom view is shown in the inset of Fig. 5.13. The reflection coefficient of the experimental prototype of ALTSA antenna is recorded using Keysight E5071C vector network analyzer. The measured reflection coefficient of the fabricated antennas is better than 13 dB within 11 GHz to 18 GHz as shown in Fig. 5.13. Furthermore, the 3D radiation pattern generated through Ansys HFSS is shown in Fig. 5.14 for the diplexer design bands 11.2 GHz and 13.85 GHz.

5.2.4 Integration of SICL based diplexer and high gain antenna & experimental validation

Diplexer integration with antenna is the first step in design of a RF-front end. Researchers have investigated various configuration to connect antenna with diplexer to facilitate frequency division as well as isolation between the transmitter and receiver channel. A novel integration of diplexer & antenna [195] for high-capacity millimeter-wave communication is proposed without the need for electrical contact between ridge gap waveguide based 7^{th} order diplexer and 16 $\times$ 16 slot array antenna. In an effort to design compact systems, a self-diplexed SIW antenna [196] was

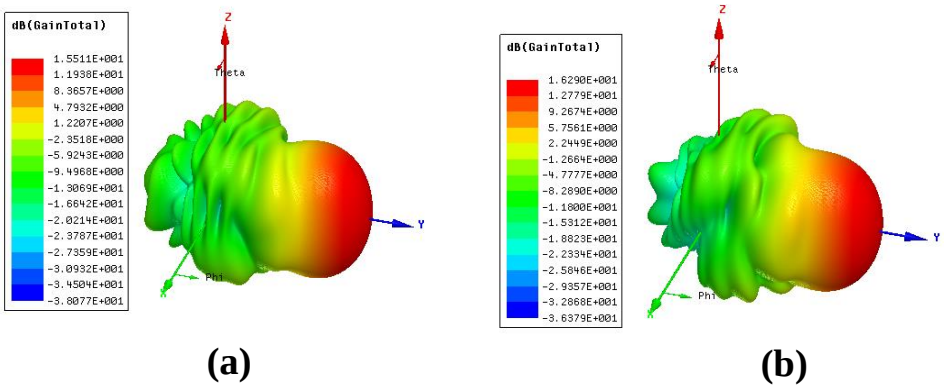

Figure 5.14 : The three-dimensional radiation pattern of the GCPW fed high gain antipodal linearly tapered slot antenna (ALTSA) at (a) 11.25 GHz (b) 13.8 GHz.

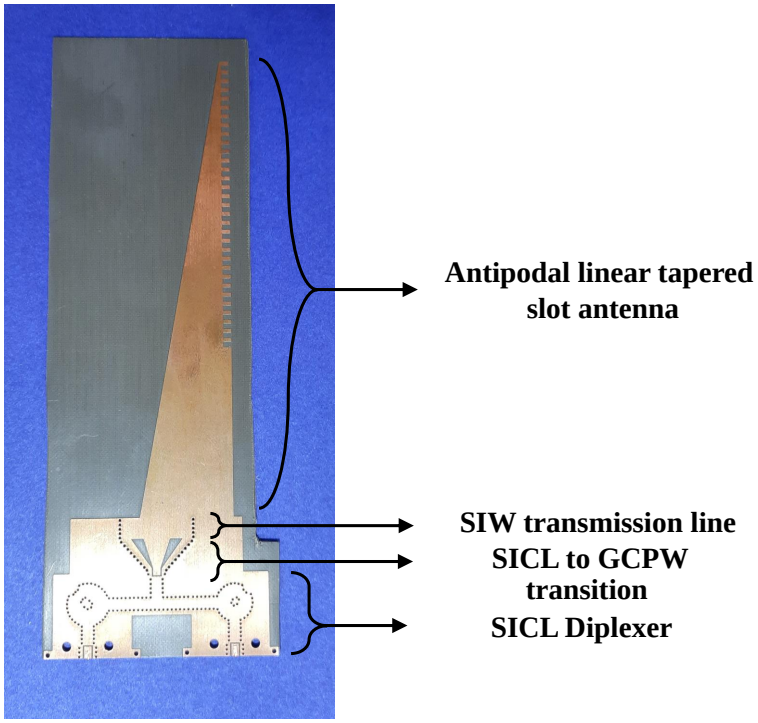

Figure 5.15 : Photograph of fabricated prototype of the SICL based diplexer-antenna integration.

conceived. While self-diplexing antennas have the ability isolate the transmitting and receiving channel, they generally suffer from poor roll-off rate for sharp rejection outside the band of operation. A fourth order bandpass filter designed using open-loop resonators has been coupled a microstrip based patch antenna [197] to form the initial section of RF-front end. A diplexer-antenna integration technique proposed in [198] utilizes bandpass filters connected to a single feed line in order to excite a multi-band microstrip antenna. Recently, SIW diplexer-antenna integration featuring high-Q factor [199, 200] has been proposed for millimeter-wave communication. Owing to advancements in stereolithography (SLA) has allowed to realize a fully 3D printed front-end consisting of a 2×2 horn antenna arrays and a K_u-band diplexer. However, there is still an evident gap for a single technology that has the capabilities to mass-produce cost efficient self-shieleded

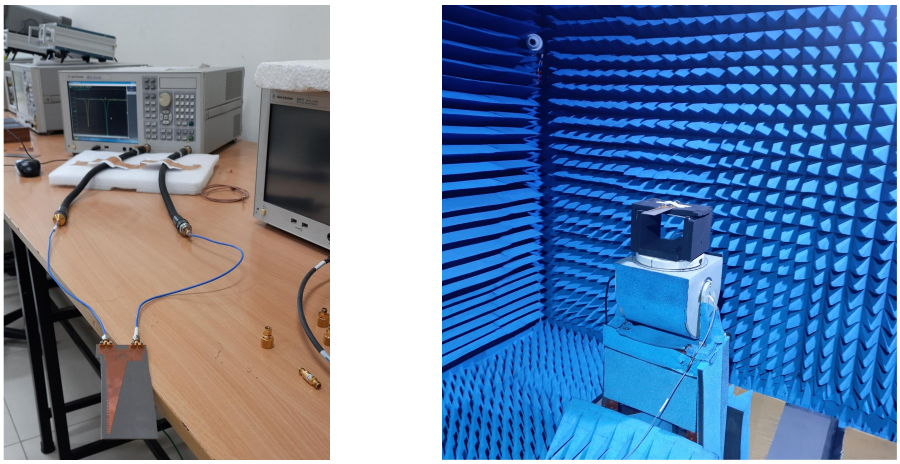

(a) (b)

Figure 5.16 : Measurement setup of proposed SICL diplexer-antenna integration (a) S-parameters measurement using VNA (b) Radiation pattern measurement in anechoic chamber

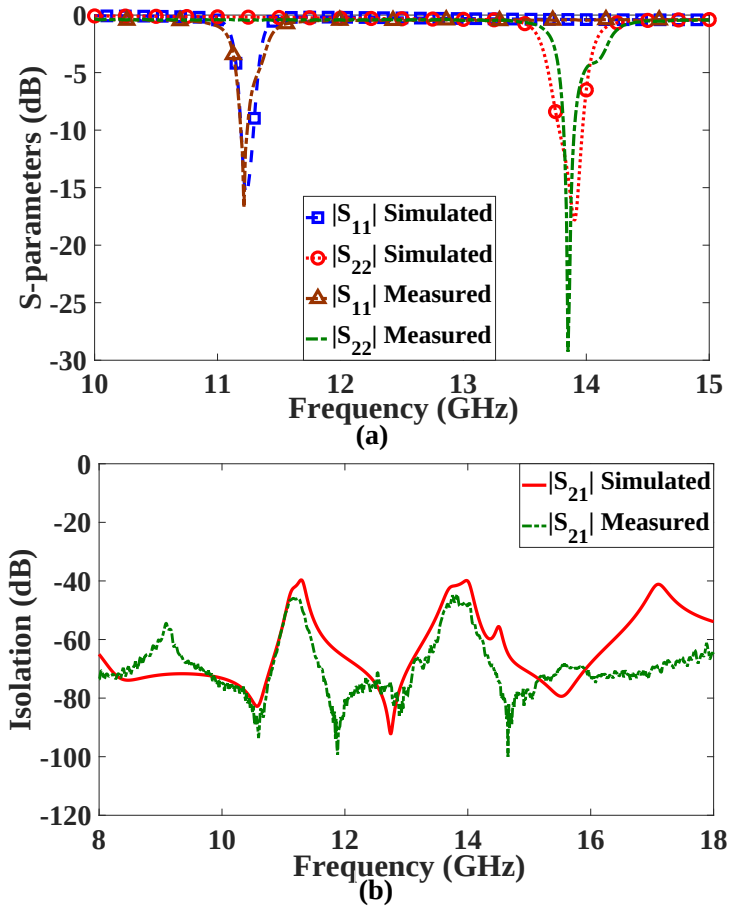

Figure 5.17 : Measured and full-wave simulated S-parameters of the final SICL diplexer and antenna integration (a) $|S_{11}|$ & $|S_{22}|$ (b) $|S_{21}|$.

compact systems with low-loss and ease of integration.
The proposed SICL diplexer is integrated with an ALTSA antenna using a SICL to GCPW transition. The SICL based diplexer is connected to a GCPW line using a metal plated blind via. This GCPW is gradually tapered in to the SIW section in order to provide a smooth transition from TEM based GCPW topology to TE_{10} mode of propagation in SIW transmission line. Finally, the out of phase currents in the SIW line is utilized to excite the ALTSA antenna.

The proposed work demonstrates seamless integration capabilities of SICL with its other planar counterparts. From a system integration point of view SICL based technology provides the much required shielding capabilities within a compact size and demonstrates ease of integration.

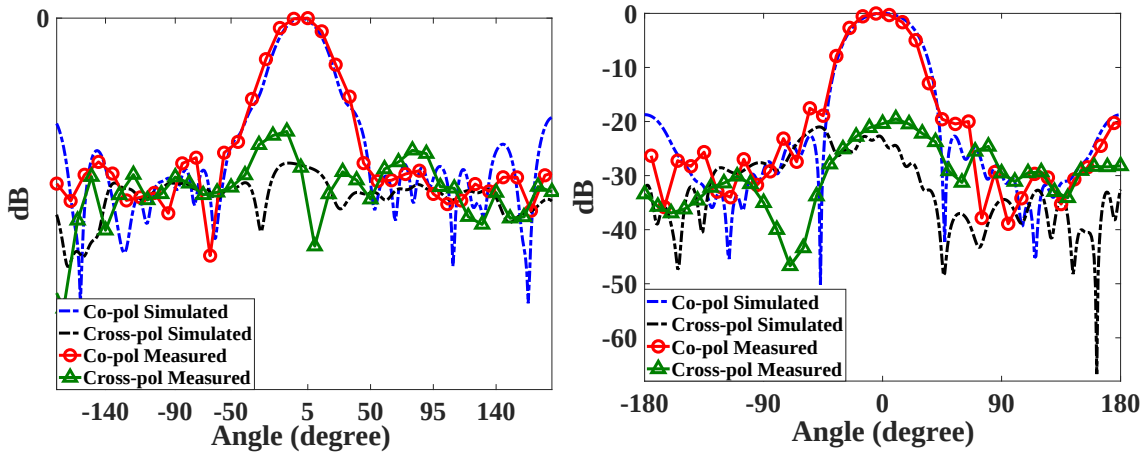

Figure 5.18 : Measured radiation pattern recorded in anechoic chamber and full-wave simulated radiation pattern observed at 11.25 GHz (a) E-plane (b) H-Plane.

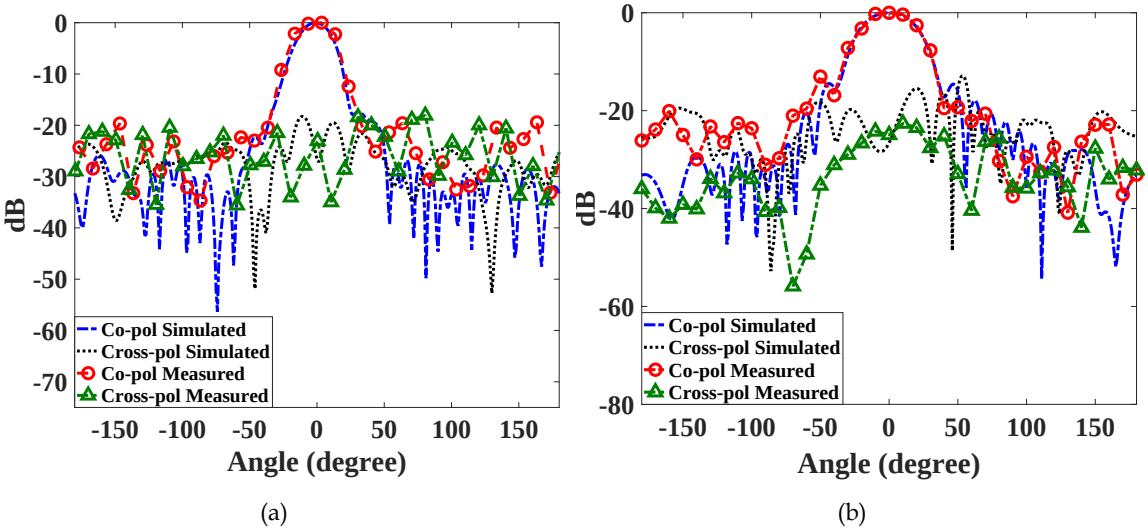

Figure 5.19 : Measured radiation pattern recorded in anechoic chamber and full-wave simulated radiation pattern observed at 13.8 GHz (a) E-plane (b) H-Plane.

The proposed diplexer-antenna integration is synthesized using multi-layered PCB technology. The photograph of the fabricated diplexer-antenna system is depicted in Fig. 5.15. The test and measurement setup for experimental validation is shown in Fig. 5.16. The reflection coefficient of the transmitting channel and receiving channel is recorded using Keysight E5071C vector network analyzer and compared with the full-wave simulated results obtained from HFSS as shown in Fig. 5.17(a). The reflection coefficient at both bands is better than 15 dB with a 10 dB bandwidth of 60 MHz and 85 GHz centered at 11.21 GHz and 13.85 GHz respectively. These two bands are prominent for on the move SATCOM applications [192]. Also, in the proposed system the measured isolation of better than 45 dB between the transmitting and receiving channel has been obtained as shown in Fig. 5.17(b). Another desirable feature of the proposed system is the excellent out of band rejection owing to the TEM based propagation. In Fig. 5.17(a) and (b) it is shown there are no excitation of higher order modes up to 20 GHz. The radiation pattern of the proposed diplexer antenna system are measured in a completely shielded anechoic chamber as shown in Fig. 5.16 (b). The proposed antenna fed by SICL diplexer exhibits a simulated gain of 14.45 dBi and 14.2 dbi at 11.25 GHz and 13.85 GHz, respectively. The measured gain of the antenna fed by SICL diplexer has a peak value of 13.8 dBi and 13.15 dBi at 11.21 GHz and 13.85 GHz, respectively. The comparison between simulated and measured E and H plane radiation pattern of the proposed diplexer-antenna is shown in Fig. 5.18 and 5.19 respectively. The measured radiation pattern of the ALTSA antenna fed by high isolation SICL based diplexer is in accordance with the full-wave simulated pattern with slight deviation due to fabrication tolerances and limitation in measurement setup. The simulated and measured cross polar level is below 27.7 dB and 28.16 dB from the co-polar component respectively at 11.21 GHz. Whereas at 13.85 GHz, the difference between simulated and measured cross-polar and co-polar component is better than 26.58 dB and 23.05 dB respectively. The simulated and measured HPBW in E-plane is 28.1° and 30.8°, respectively compared to simulated and measured HPBW of 48° and 46.8° respectively, in-plane at 11.21 GHz . Similarly, the simulated and measured HPBW in E-plane is 27° and 29.2°, respectively compared to measured HPBW of 41.5° and 44.2° respectively, in H-plane at 13.85 GHz.

5.3 SUBSTRATE INTEGRATED COAXIAL LINE BASED WIDEBAND SIX PORT NETWORK FOR K_U APPLICATION

The first report of six-port network [201] was in 1972 by GF Engen which was developed for power measurement and calibration. Advancements in planar microwave guiding media has helped the six-port network to be explored for a variety of applications with ease of fabrication and in a compact size. Six-port network is very popular in design of RF receiver architecture such as super-heterodyne or homodyne receivers as it is developed using mostly passive components. Since it is built using all passive components it does not require any DC supply. Since passive components have much higher linearity and dynamic range than active components six-port receiver provide the best phase accuracy among receiver. Moreover six-port networks finds application in microwave imaging for all weather monitoring. Six port network does vector addition of RF and LO and does not require mixer as the detector does the frequency translation job by working in square law region. Though the six-port network is tried in several configurations it is commonly designed using a Wilkinson power divider and three branch-line couplers. The network consists of two inputs for RF and LO each, and four outputs ports. These output ports are connected to detectors that provide DC voltage as end output. The lack of wideband and completely shielded six-port network with low amplitude/phase imbalance in a compact planar form factor motivates to design a six-port network in SICL technology. Six-port passive networks occupy large foot print and hence not widely used at lower frequencies. Moreover existing solutions do not support good electromagnetic compatibilty for densely integrated systems in planar form.

The proposed SICL based six-port network is designed using one wide-band wilkinson power divider and three wideband branch line coupler that operate over the entire K_u-band as shown in

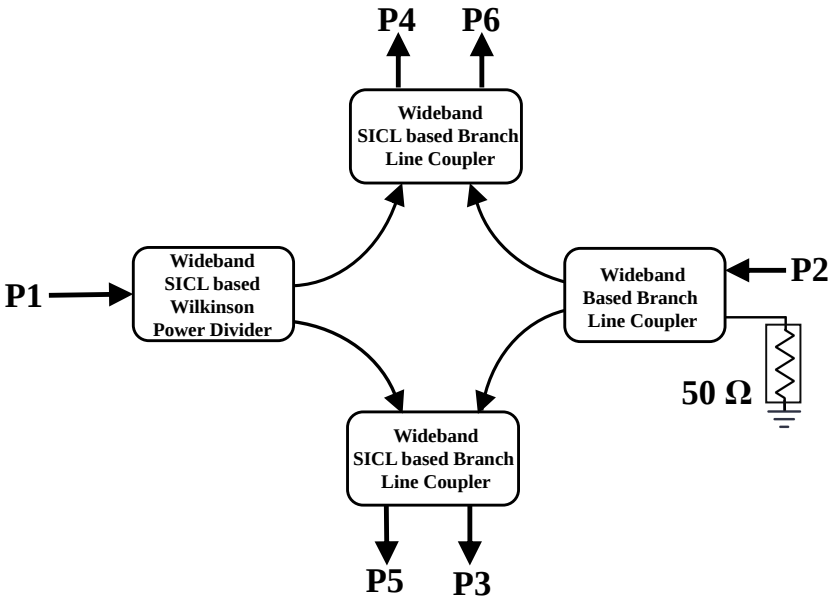

Figure 5.20 : Integration scheme of the proposed SICL based wideband six-network.

Fig. 5.20. The S-parameters of a equal split wilkinson power divider is given as (5.9)

$$[S] = \begin{bmatrix} 0 & -\frac{j}{\sqrt{2}} & -\frac{j}{\sqrt{2}} \\ -\frac{j}{\sqrt{2}} & 0 & -\frac{j}{\sqrt{2}} \\ -\frac{j}{\sqrt{2}} & -\frac{j}{\sqrt{2}} & 0 \end{bmatrix} \tag{5.9}$$

And the S-parameters of a 3 dB branch line coupler is given as equation (5.10)

$$[S] = \begin{bmatrix} 0 & -\frac{j}{\sqrt{2}} & -\frac{1}{\sqrt{2}} & 0 \\ -\frac{j}{\sqrt{2}} & 0 & 0 & -\frac{1}{\sqrt{2}} \\ -\frac{1}{\sqrt{2}} & 0 & 0 & -\frac{j}{\sqrt{2}} \\ 0 & -\frac{1}{\sqrt{2}} & -\frac{j}{\sqrt{2}} & 0 \end{bmatrix} \tag{5.10}$$

Assuming all six-ports are perfectly matched, the relation between reflected wave (b_n, where n = 1 to 6) and incident wave (a_n, where n = 1 to 6) is expressed as

$$\begin{aligned} b_1 &= 0 \\ b_2 &= 0 \\ b_3 &= \frac{a_1}{2} j + \frac{a_2}{2} j \\ b_4 &= -\frac{a_1}{2} + \frac{a_2}{2} j \\ b_5 &= -\frac{a_1}{2} + \frac{a_2}{2} \\ b_6 &= \frac{a_1}{2} j - \frac{a_2}{2} \end{aligned} \tag{5.11}$$

The S-parameters of six-port network developed using wilkinson power divider and branch line coupler can be computed using (5.12)

$$[b] = [S] \cdot [a] \tag{5.12}$$

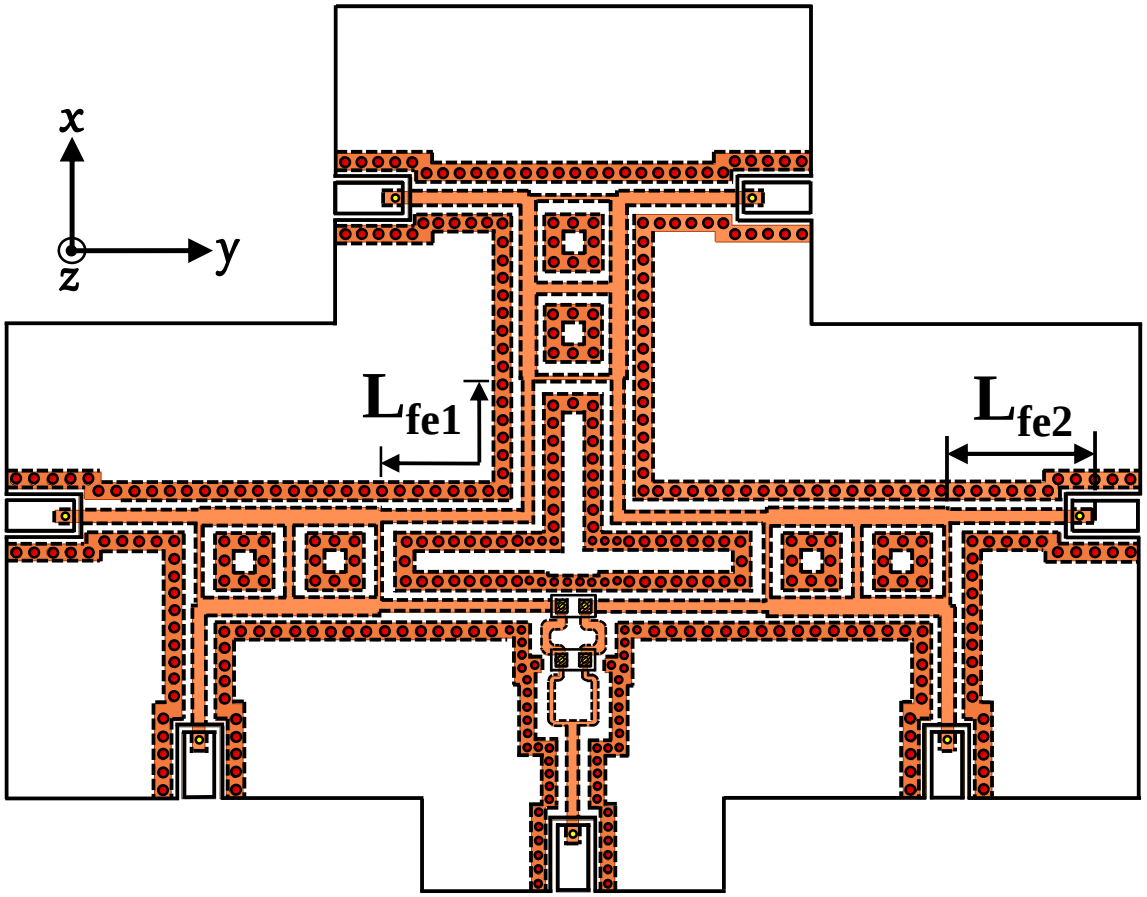

Figure 5.21 : Final geometrical layout of the proposed SICL based wideband six-port network after integration of couplers with power divider.

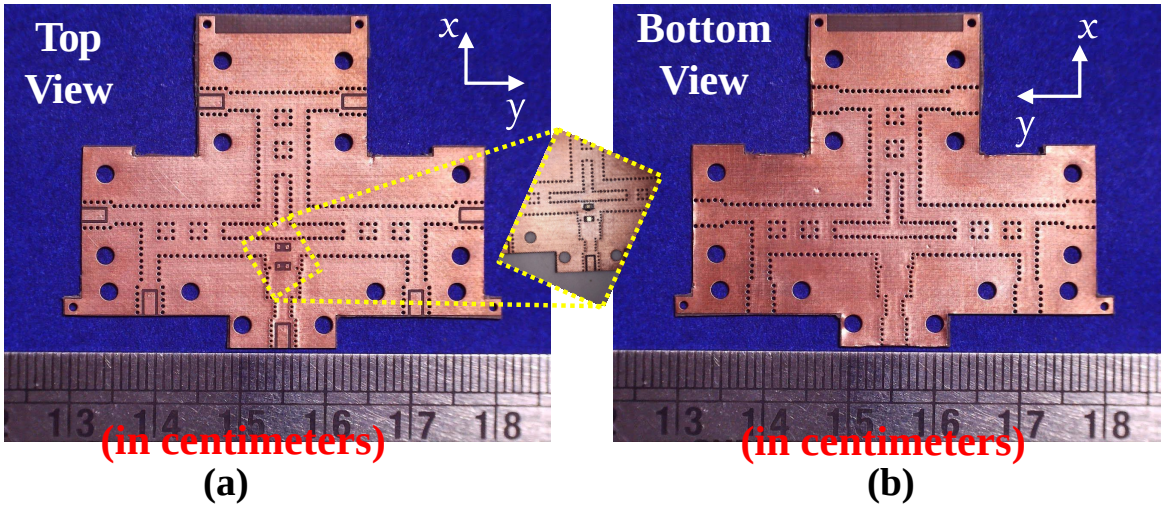

Figure 5.22 : Photograph of fabricated compact SICL based wideband six-port network for Ku-band application (a) Top -view with mounting of SMD resistor (b) Bottom view.

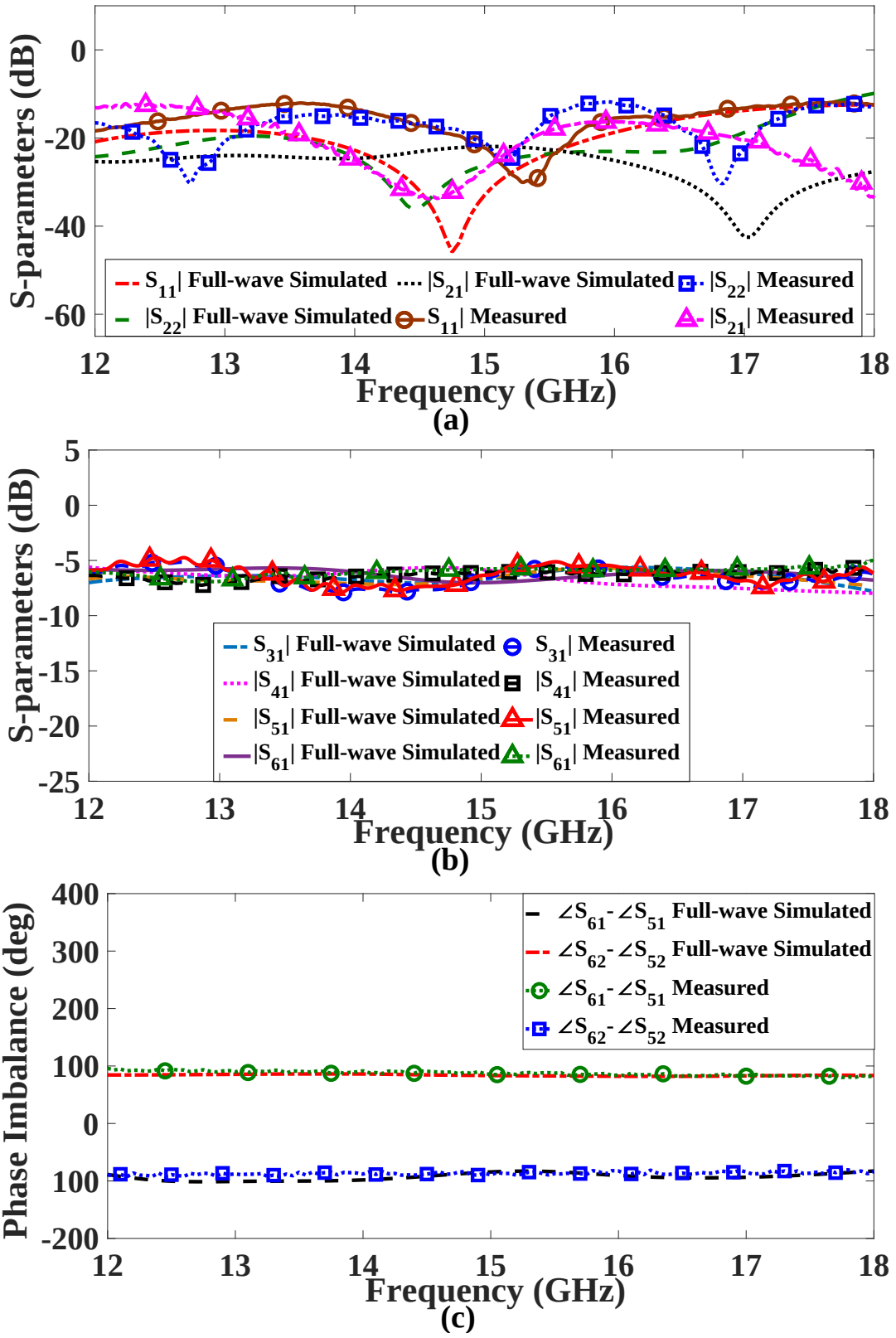

Figure 5.23 : Comparison between measured and full-wave simulated S-parameters of the proposed compact wideband six-port network (a) Reflection and isolation of input port $|S_{11}|$, $|S_{21}|$ & $|S_{22}|$ (b) Transmission from RF and LO port to output ports (c) Phase difference.

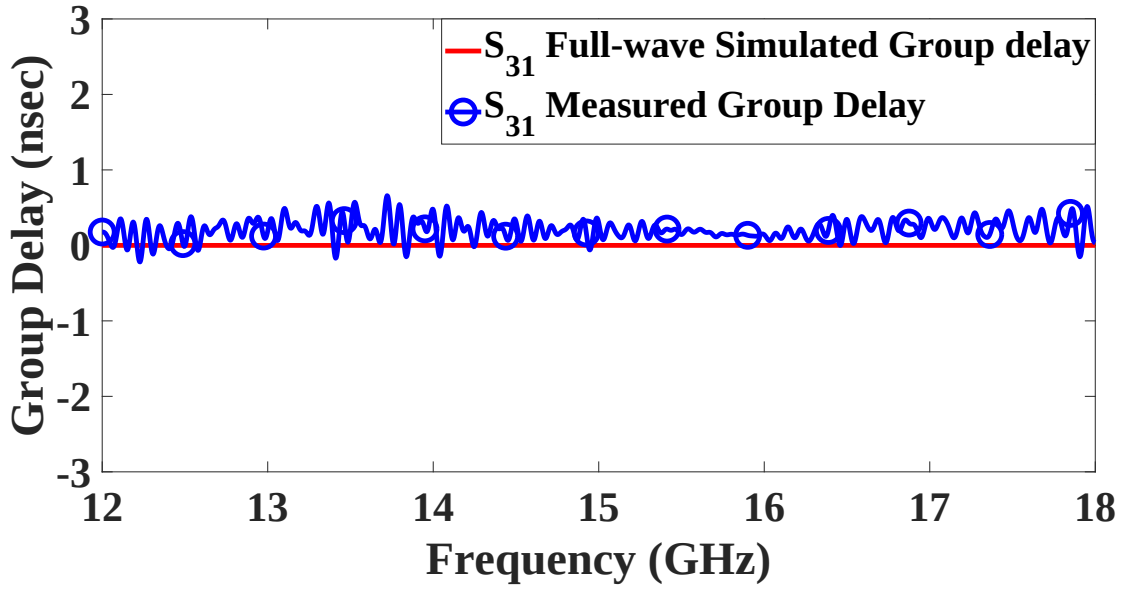

Figure 5.24 : Measured and full-wave simulated group delay of the proposed six-port network covering K_u-band.

$$\begin{bmatrix} b_1 \\ b_2 \\ b_3 \\ b_4 \\ b_5 \\ b_6 \end{bmatrix} = \begin{bmatrix} 0 & 0 & \frac{1}{2}e^{j90^\circ} & \frac{1}{2}e^{j180^\circ} & \frac{1}{2}e^{j180^\circ} & \frac{1}{2}e^{j90^\circ} \\ 0 & 0 & \frac{1}{2}e^{j90^\circ} & \frac{1}{2}e^{j90^\circ} & \frac{1}{2}e^{j0^\circ} & \frac{1}{2}e^{j180^\circ} \\ \frac{1}{2}e^{j90^\circ} & \frac{1}{2}e^{j90^\circ} & 0 & 0 & 0 & 0 \\ \frac{1}{2}e^{j180^\circ} & \frac{1}{2}e^{j90^\circ} & 0 & 0 & 0 & 0 \\ \frac{1}{2}e^{j180^\circ} & \frac{1}{2}e^{j0^\circ} & 0 & 0 & 0 & 0 \\ \frac{1}{2}e^{j90^\circ} & \frac{1}{2}e^{j180^\circ} & 0 & 0 & 0 & 0 \end{bmatrix} \cdot \begin{bmatrix} a_1 \\ a_2 \\ a_3 \\ a_4 \\ a_5 \\ a_6 \end{bmatrix} \tag{5.13}$$

5.3.1 Design and development of proposed Six-port network

The working, fabrication and testing of branch line coupler & power divider in SICL technology has been discussed in detail section 4.5 and 4.8 respectively of chapter 4. SICL is a two conductor transmission line. The lateral metallic vias along with bottom and top ground plane form outer conductor, whereas the metallic strip sandwiched between the substrate makes the inner conductor of this planar dielectric filled coaxial line. The coaxial like radially outward directed E-field vector and concentric H-field in SICL transmission line are confirmed using Ansys HFSS and their field distribution has been shown in Fig. 1.5. The final geometrical layout of the proposed six-port network in SICL technology designed for K_u-band in Fig. 5.21 and the photograph of the proposed SICL based wideband six-port network fabricated using Taconic TLY-5 (ε_r = 2.2, δ = 0.0009) with thickness 0.254 mm for the upper and lower substrate and Taconic FR-28 as prepeg (ε_r = 2.74, tanδ = 0.0014) is shown in Fig. 5.22. The full-wave simulated response generated using Ansys HFSS is confirmed by measuring the S-parameters of proposed prototype using Agilent E5071C vector network analyzer as shown in Fig. 5.23. Measured return loss and isolation at the input port of the compact wideband six-port network ($|S_{11}|$, $|S_{21}|$ & $|S_{22}|$) is better than 10 dB over the entire range of 12 GHz to 18 GHz. Further, the measured transmission from RF and LO port to output ports is within an imbalance of $\pm$1.6 dB. Whereas the measured phase imbalance is better than $\pm 8^\circ$. Finally, owing to the non-dispersive behavior of SICL, low measured group delay variation with peak group delay of 0.56 ns is shown in Fig. 5.24. The proposed invention reports a completely shielded and self-packaged six- port network in substrate Integrated Coaxial Line (SICL) technology that supports a wide-bandwidth covering the entire

K_u-band (12 GHz to 18 GHz) in a highly compact form factor.

5.4 CONCLUDING REMARKS

This chapter discusses the design and fabrication of multi-functional SICL components and integration of passive components to design diplexer-antenna and a six-port receiver. Firstly, an SICL based multi-functional component demonstrating both radiating and filtering function has been realized. The initial design comprised of a 5^{th}-order bandpass filter designed and fabricated in SICL based technology. The filter synthesis is affirmed by fabricating an experimental prototype. The measured results of proposed SICL bandpass filter demonstrates an insertion loss of 1.96 dB at the center frequency 28 GHz with a 3-dB fractional bandwidth of 14.03%. A technique to integrate slot antenna over the filter has been proposed to realize the filtering antenna. The peak gain of co-designed filter-antenna is better than 4.8 dBi at 25.45 GHz with good selectivity. Instead of cascading the front-end components, proposed co-design approach in SICL technology can maintain compact size as the slot antenna is situated over filtering element and eliminates the need for any interface between filter & antenna. The proposed SICL filter-antenna is a good candidate for millimeter-wave transceivers.

The next work deals with the design and development of a highly selective diplexer with high isolation owing to the multiple transmission zeros of the synthesized bandpass filters. The proposed diplexer conceived by two SICL based via-perturbed bandpass filters and an impedance matching network exhibits low insertion loss and excellent out of band rejection. The proposed SICL based diplexer exhibits low insertion loss of 1.33 dB and 1.58 dB at the center frequency 11.2 GHz and 13.8 GHz respectively. Utilization of highly selective filters with selectivity as high as 106.2 dB/GHz and multiple transmission zeros aids in achieving steep rejection skirt as well as excellent out of band rejection. The self-shielded structure of SICL and multiple transmission zeros outside the band of operation provides a high measured isolation greater than 45 dB at both transmit and receive bands of the proposed diplexer. A wideband high gain linearly tapered antipodal antenna fed by GCPW line is realized covering a frequency range of 11 GHz to 18 GHz. The SICL diplexer-antenna integrated system has a measured gain of the peak value of 13.8 dBi and 13.15 dBi at 11.21 GHz and 13.85 GHz, respectively. The integration of the proposed diplexer with a high gain antenna is of immense interest in design of commercial RF front-end.

Finally, using the wideband branch line coupler and wideband wilkinson power divider a completely self-packaged and self-shielded SICL based six-port module is designed, fabricated and experimentally validated. The proposed wideband six-port network works over the entire K_u band with low group delay is realized in a compact form factor. A measured return loss and isolation at the input port of the compact wideband six-port network is better than 10 dB over the entire range of 12 GHz to 18 GHz and the measured transmission from RF and LO port to output ports is within an imbalance of $\pm$1.6 dB. To summarize, this chapter essentially demonstrates advantages of SICL technology in realizing microwave/ millimeter-wave components in a compact form factor with low-loss propagation, and ease of integration to design various RF front-end components with enhanced functionalities.

…